First-principles rheological modelling and parameter estimation for nanoparticle-based smart drilling fluids

Zdravko Kravanja (Editor), Proceedings of the 26th European Symposium on Computer-Aided Process Engineering – ESCAPE 26
June 12th -15th, 2016, Portorož, Slovenia

First-principles Rheological Modelling and Parameter Estimation for Nanoparticle-based Smart Drilling Fluids

Simon I. Reilly,[a] Zisis Vryzas,[b] Vassilios C. Kelessidis,[b] Dimitrios I. Gerogiorgis[a]

[a] *School of Engineering (IMP), University of Edinburgh, Edinburgh EH9 3FB, UK*
[b] *Petroleum Engineering Program, Texas A&M University at Qatar, Doha, Qatar*

Abstract
Drilling fluids serve many applications in the oil-drilling process, including the removing of cuttings, drill bit cooling and the prevention of fluid transfer to and from the rock strata. With the addition of nanoparticles it is possible to facilitate in-situ control of the drilling fluid rheology, increasing the hydraulic efficiency of drilling campaigns and reducing costs in a variety of reservoir environments. This paper proposes a first-principles approach to the rheology of smart drilling fluids containing Fe_3O_4 nanoparticles which have shown advantages to increasing drilling efficiency in a variety of reservoir environments. The model for shear stress is developed based on a force balance between the Van der Waals attractions of monodispersed Fe_3O_4 nanoparticle spheres. The model for viscosity is developed by considering the force required to maintain the nanoparticles in suspension being equal to the drag force as calculated for Stokes flow approximation about a sphere. Both models had a candidate equation for interparticle distance under increasing shear rate. A bivariate model described the rheological effects of shear rate and Fe_3O_4 nanoparticle concentration with a high predictive potential ($R^2_{\tau(\dot{\gamma},\phi)}$ = 0.993, $R^2_{\mu(\dot{\gamma},\phi)}$=0.999). The trivariate model accounts for temperature with high predicative potential ($R^2_{\tau(\dot{\gamma},\phi,T)}$ = 0.983, $R^2_{\mu(\dot{\gamma},\phi,T)}$ =0.986). Heating effects and low nanoparticle concentrations increase standard correlation error.

Keywords: nanoparticles, drilling fluids, rheology, modelling, shear stress, viscosity.

1. Introduction
Applications of smart drilling fluids facilitate in-situ control of fluid rheology, making their transport properties tunable. This benefits their application in different down-hole environments, where differing technical and economic challenges arise. A nanofluid can perform several tasks in the fluid system, and facilitate drilling with a reduction in total solid and/or chemical content of the equivalent mud, whilst also reducing costs (Amanullah & Al-Tahini, 2013). The development of first principle models for rheology of nanofluids, which can characterise the fluid behaviour as a function of shear rate ($\dot{\gamma}$), nanoparticle volume fraction (ϕ) and temperature (T), is critical toward modelling, design and planning of cost effective drilling campaigns. Upon successful validation, these models have general applicability to all function forms of nanoparticle-enhanced drilling fluids, eliminating the need for parameterised approximations of fluid rheology.

Previous investigations into the behaviour of drilling muds have revealed a strong non-Newtonian behaviour with muds exhibiting a yield stress and shear thinning (Kelessidis & Maglione, 2008). The presence of aggregates in the nanofluid, which are destroyed under high shear, gives a possible description of the observed behaviour. The objective of the present study is to quantify the rheology of the fluid by developing expressions which describe the phenomena evolving in nanofluids (Zhou et al., 2010).

2. First Principle Model Development

The first-principles models assume monodisperse spherical Fe_3O_4 nanoparticles suspended in a continuous bentonite drilling fluid: the interaction between nanoparticles considers only Van der Waals forces by virtue of an isoelectric point (IEP) assumption.

2.1. Shear Stress model

The equation for the shear stress of bentonite drilling mud containing Fe_3O_4 nanoparticles was developed by considering the summation of three physical quantities.

$$\tau = \tau_y + \tau_\eta + \tau_{VdW} \tag{1}$$

The yield stress of the suspension (τ_y) and shear stress at limiting viscosity (τ_η), were obtained from a previous experimental campaign (Gerogiorgis et al., 2015). The additional interaction stress (τ_{VdW}) is proportional to the magnitude of the Van der Waals forces which are exerted between the nanoparticles. After yielding, the suspension contains nanoparticle aggregates, idealised as doublets (Flatt & Bowen, 2007). Pouyafar and Sadough (2013) suggested a further breakdown in the percolating nanoparticle isostructure under increasing shear rate; on this assumption we postulate a shear dependent average interparticle distance. It is assumed that the nanoparticle doublets are cubically distributed, increasing shear rate disperses particles into a final cubic distribution, with fixed interparticle distance (δ) which is a function of nanoparticle volume fraction as shown by Eq. (2) (Masoumi et al., 2009). A quasi-equilibrium condition is applied to the shear-dependant structuring term (λ_τ) in Eq. (3) (Pouyafar & Sadough, 2013). The role of the percolation threshold volume fraction (ϕ_o), at which long-range connectivity is observed, is considered in the structuring term (Flatt & Bowen, 2006). An average interparticle distance (H_τ) is expressed in Eq. (4) as a function of the minimum and maximum shear limits of interparticle distance. The Van der Waals force (F_{VdW}) in the absence of an intervening medium includes the haymaker constant (A_o) as shown in Eq. (5). Stress associated with the attraction force acts across the nanoparticle surface (A_p) thus Eq. (6) gives the interaction stress and Eq. (7) is the broad form of the shear stress equation. Bivariate and trivariate models consider base fluid viscosity (μ_{bf}): Eqs. (8-9) are fitted to experimental data (Gerogiorgis et al., 2015).

$$\delta = d_p \sqrt[3]{\frac{\pi}{6\phi}} \tag{2}$$

$$\lambda_\tau = \frac{1}{1+\phi_o \dot{\gamma}} \tag{3}$$

$$H_\tau = \delta(1-\lambda_\tau) + 2\delta\lambda_\tau \tag{4}$$

$$F_{VdW} = \frac{r_p A_o}{12 H_\tau^2} \tag{5}$$

$$\tau_{VdW} = \frac{r_p A_o}{12 H_\tau^2 A_p} \tag{6}$$

$$\tau = \tau_y + \frac{r_p A_o}{12 H_\tau^2 A_p} + \eta_\infty \dot{\gamma} \tag{7}$$

$$\tau = \tau_y + \alpha\left(\frac{r_p A_o}{12 H_\tau^2 A_p}\right) + \beta\mu_{bf}\dot{\gamma} \tag{8}$$

$$\tau = \tau_y + (\alpha T - \beta)\left(\frac{r_p A_o}{12 H_\tau^2 A_p}\right) + \exp\left(\frac{\kappa}{T}\right)\mu_{bf}\dot{\gamma} \tag{9}$$

2.2. Viscosity Model

An independent equation for the viscosity of bentonite based smart drilling fluids is proposed. The principal assumption is that the apparent viscosity (μ_{app}) is the sum of the base fluid viscosity and the effective viscosity due to nanoparticle interactions within the fluid (μ_{eff}); contributions can then be considered separately (Masoumi et al., 2009).

$$\mu_{app} = \mu_{bf} + \mu_{eff} \tag{10}$$

The equation for the effective viscosity of bentonite drilling mud containing Fe_3O_4 nanoparticles is constructed on a similar interparticle distance assumption as the shear stress model. The shear dependent structuring term (λ_μ) in Eq.(11) does not consider long range interaction, disregarding the percolation threshold, to express the average doublet separation distance (H_μ) in Eq.(12). The zero shear rate doublet separation distance (h_o) is assumed to be two nanoparticle diameters. Shear is assumed to increase separation to cubic packing as shown for the shear stress model. The shear rate experienced by a particle ($\dot{\gamma}_p$) from Eq.(13) gives the nanoparticles rotational velocity (u_p) as shown in Eq.(14) (Krieger & Dougherty, 1959). A drag force (F_D) is experienced by each particle, which is proportional to the free stream velocity due to particle rotation. The Reynolds numbers of particle rotation are of the correct magnitude for a Stokes flow approximation (Re << 1). The solution for drag acting on a small spherical particle in Stokes flow is Eq.(15), and it is set equal to the Van der Waals attraction force to give the effective viscosity. The drilling fluids considered have a base fluid of water, it was found that using this viscosity produced a poor representation of the rheological experimental data. The limiting viscosity of the nanoparticle suspension (η_∞) replaces the base fluid viscosity in Eq.(10) and is determined from the point of maximum shear rate, where viscosity approaches a constant value. By substituting Eq.(16) into Eq.(10), the apparent viscosity of the fluid was accounted for, giving Eq.(17) which is a function of shear rate and nanoparticle volume fraction. The final component required for the trivariate model given by Eq.(18) was an Arrhenius-form temperature relation, as developed in the previous study by Gerogiorgis et al. (2015). The values of β and E are computed numerically by employing a least-square regression methodology, using a previously given experimental dataset (Gerogiorgis et al., 2015).

$$\lambda_\mu = \frac{1}{1+\dot{\gamma}} \tag{11}$$

$$H_\mu = h_o\lambda_\mu + \delta\left(1-\lambda_\mu\right) \tag{12}$$

$$\dot{\gamma}_p = \frac{\dot{\gamma}}{2} \tag{13}$$

$$u_p = r_p\dot{\gamma}_p \tag{14}$$

$$F_D = 6\pi\mu_{eff}r_p u_p \tag{15}$$

$$\mu_{eff} = \frac{A_o}{72\pi\dot{\gamma}_p r_p H_\mu^2} \tag{16}$$

$$\mu_{app} = \eta_\infty + \beta\frac{A_o}{72\pi\dot{\gamma}_p r_p H_\mu^2} \tag{17}$$

$$\mu_{app} = \eta_\infty + \beta e^{-\frac{E}{RT}}\frac{A_o}{72\pi\dot{\gamma}_p r_p H_\mu^2} \tag{18}$$

3. Results and Discussion

3.1. Bivariate viscosity and shear stress models

Our viscosity and shear stress correlations for all temperatures appear in Figure 1.

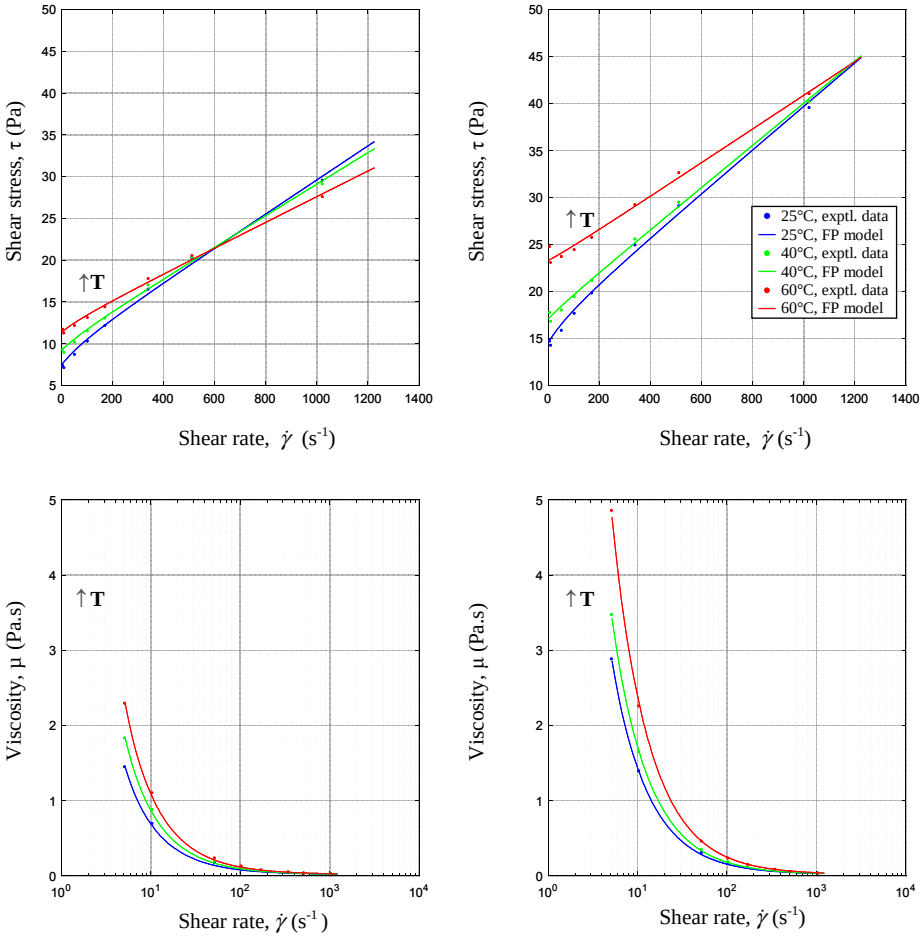

Figure 1: Shear stress vs. shear rate (upper left ϕ = 0.005; upper right ϕ = 0.03) and viscosity vs. shear rate (lower left ϕ = 0.005; lower right ϕ = 0.03for all campaign temperatures.

The nonlinear plots generated by the first-principle interparticle distance models show good agreement with experimental data for shear stress and viscosity. The upward trend in shear stress with increasing shear rate fits accurately to the model. There was clearly defined shear thinning supported by a reduction in gradient with increasing shear rate. Comparison of the shear stress plots for upper left ϕ = 0.005 and ϕ = 0.03 shows that temperature effects affect rheological behaviour with increasing nanoparticle volume fraction. The trend in decreasing viscosity with shear rate is in accordance with the observed shear thinning behaviour from the experimental campaign (Gerogiorgis et al., 2015). The model predicted a continuous increase in shear stress and apparent viscosity with greater nanoparticle volume fraction. This agreed with the experimental data. Increasing temperature produced greater viscosity in the drilling fluid which was contrary to expectations; this phenomena was confirmed in literature (Annis, 1967).

Table 1: Parameter estimation for bivariate viscosity and shear stress models.

			τ			μ		
ϕ	T (°C)	α	β	R^2	*RMSE*	β	R^2	*RMSE*
0.005	25	31.31	22.59	0.9961	0.4564	24.35	0.9986	0.0178
	40	18.96	20.95	0.9968	0.3677	30.96	0.9991	0.0177
	60	15.25	17.08	0.9957	0.3462	38.75	0.9995	0.0178
0.01	25	15.77	23.29	0.9974	0.3730	18.33	0.9988	0.0190
	40	6.348	17.13	0.9968	0.2951	19.87	0.9998	0.0076
	60	4.659	14.95	0.9943	0.3425	25.62	0.9999	0.0087
0.015	25	14.21	23.97	0.9957	0.5023	18.08	0.9996	0.0144
	40	9.549	20.97	0.9959	0.4185	21.99	0.9997	0.0148
	60	0.8180	16.95	0.9938	0.3920	29.88	0.9999	0.0050
0.02	25	15.42	25.59	0.9952	0.5756	19.63	0.9995	0.0208
	40	5.720	25.31	0.9964	0.4636	22.70	0.9998	0.0147
	60	–0.1765	20.99	0.9957	0.4020	29.70	0.9999	0.0071
0.03	25	10.31	25.69	0.9949	0.5904	16.56	0.9986	0.0138
	40	2.861	25.00	0.9972	0.3938	19.89	0.9993	0.0154
	60	–1.898	20.10	0.9887	0.6100	27.70	0.9998	0.0299

3.2. Trivariate viscosity and shear stress models

The trivariate models for shear stress and viscosity are presented in Figure 2.

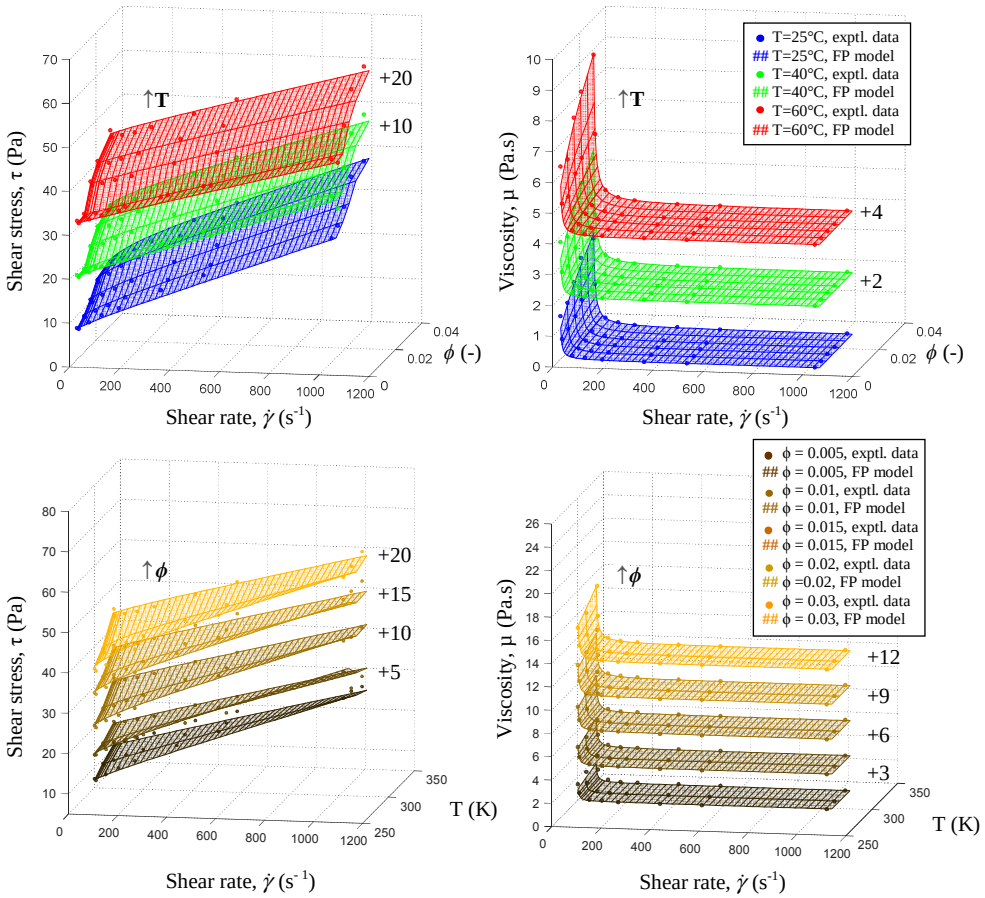

Figure 2: Trivariate model plots for all experimental campaigns: shear stress (left) and viscosity (right) at constant temperature intervals (top) and constant nanoparticle volume fractions (bottom).

At low shear rates, particle volume fraction has greater effect on the viscosity and shear stress. At high volume fractions, the temperature effects become more dominant in characterizing the upward trend in shear stress, leading to discrepancies between models and experimental data.

Table 2: Parameter estimation for trivariate viscosity and shear stress models.

			τ				μ		
***T* (°C)**	α	β	κ	R^2	*RMSE*	β	E	R^2	*RMSE*
25	–0.3664	–126.8	935.4	0.9908	0.8057	1642	–1352	0.9846	0.0921
40	–0.3664	–126.8	935.4	0.9767	1.1910	1642	–1352	0.9813	0.1210
60	–0.3664	–126.8	935.4	0.9847	0.9014	1642	–1352	0.9885	0.1278

4. Conclusions

Our first-principles rheological model for smart drilling fluids was based on shear dependant interparticle distance. A structuring term described the change from a percolating nanoparticle isostructure, to a cubic distribution of nanoparticles, with an approximation to Newtonian flow at high shear rates. Bivariate and trivariate models were fitted to experimental data by least square regression at Fe_3O_4 nanoparticle volume fractions 0.005, 0.01, 0.015, 0.02, and 0.03 (Gerogiorgis et al., 2015). The bivariate model described the rheological effects of shear rate and nanoparticle concentration, with high predictive potential ($R^2_{\tau(\dot{\gamma},\phi)}$ = 0.993, $R^2_{\mu(\dot{\gamma},\phi)}$=0.999). The trivariate model described the rheological effects of shear rate, nanoparticle concentration, and temperature producing a high predictive potential ($R^2_{\tau(\dot{\gamma},\phi,T)}$ = 0.983, $R^2_{\mu(\dot{\gamma},\phi,T)}$ =0.986). Heating effects and low nanoparticle concentrations also increase standard error further.

Acknowledgement

The present publication has been made possible by NPRP Grant Number 6-127-2-050 from Qatar National Research Fund, QNRF (a member of the Qatar Foundation). The statements which have been made herein are solely the responsibility of the authors.

References

B. Abu-Jdayil, M. Ghannam, 2014, *Energ. Source Part A*, 36(10), 1037–1048.
M. Amanullah, A.M. Al-Tahini, 2013, *Proc. SPE Saudi Arabia Tech. Symp. Soc. Petrol. Eng.*
J. Andertová, F. Rieger, 2009, *Ceram. Sil.*, 53, 283–286.
M.R. Annis, 1967, *J. Petrol. Technol.*, 19(8), 1074–1080.
N.J. Balmforth et al., 2014, *Annu. Rev. Fluid Mech*, 46(1), 121–146.
J.M. Berge, 1993, *Least squares optimilzation in multivariate analysis.* DSWO Press.
A.Y. Dandekar, 2013, *Petroleum Reservoir Rock and Fluid Properties.* Taylor & Francis.
R.J. Flatt, P. Bowen, 2006, *J. Am. Ceram. Soc.* 89(4), 1244–1256.
R.J. Flatt, P. Bowen, 2007, *J. Am. Ceram. Soc.* 90(4), 1038–1044.
D.I. Gerogiorgis et al., 2015, *Comput. Aided Chem. Eng.* 37(1), 2405-2410.
F.A. Graybill, 1994, *Regression Analysis: Concepts and Applications*. Duxbury Press.
J. Hermoso et al., 2012, *Ind. Eng. Chem. Res.*, 51(44), 14399–14407.
V.C. Kelessidis et al., 2006, *J. Petrol. Sci. Eng.*, 53(3–4), 203–224.
V.C. Kelessidis, R. Maglione, 2008, *Colloid Surface A*, 318(1–3), 217–226.
I.M. Krieger, T.J. Dougherty, 1959, *T. Soc. Rheol.*, (1957–1977), 3(1), 137–152.
N. Masoumi et al., 2009, *J. Phys. D Appl. Phys.*, 42(5), 055501.
V. Pouyafar, S.A. Sadough, 2013, *Metal. Mater. Trans. B*, 44(5), 1304–1310.
G. Puxty et al., 2006, *Chemometr. Intell. Lab*, 81(2), 149–164.
Q.D. Nguyen, D.V. Boger, 2003, *Annu. Rev. Fluid Mech*, 24(1), 47-88
J.J. Sheng, 2011, *Modern Chemical Enhanced Oil Recovery - Theory and Practice* . Elsevier.
M. Waheed, 2013, *Technical Report*, Texas A&M University, Doha.
J. Yan, A.E. James, 1997, *J. Non-Newton Fluid.*, 70(3), 237–253.
S.Q. Zhou et al., 2010, *J. Appl. Phys.*, 107(5), 054317.